

# Direct Imprinting of Microelectrodes for High-Performance Miniature Power Sources

Wenhao Li,<sup>1</sup> Vince Einck,<sup>1</sup> Cheng Li,<sup>1</sup> Yiliang Zhou,<sup>1</sup> Troels Christiansen,<sup>2</sup> Bo B. Iversen<sup>2</sup> and James J. Watkins<sup>1</sup>

Department of Polymer Science and Engineering, University of Massachusetts<sup>1</sup>  
Amherst, MA USA 01003

Department of Chemistry, Aarhus University<sup>2</sup>

Langelandsgade 140, Aarhus, Denmark

E-mail: [watkins@polysci.umass.edu](mailto:watkins@polysci.umass.edu)

Microbatteries with form factors comparable to MEMS *e.g.*, microsensors and actuators, offer exciting opportunities to achieve self-powered, all-on-one-chip devices. Despite significant advances of the 3D microbattery theories, scalable fabrication of microelectrodes with complicated 3D architectures and the assembly of miniature components into a well-functioning battery remain elusive. Here we utilize soft imprint lithography and functional nanoparticle inks, including  $\text{LiMn}_2\text{O}_4$  (LMO),  $\text{Li}_4\text{Ti}_5\text{O}_{12}$  (LTO) and  $\text{TiO}_2$ , to fabricate high aspect ratio microelectrodes. The nanoparticles, either commercial or home-synthesized, bear sub-20 nm diameters, rendering fine and stable dispersions for imprinting and offering significant advantages for easy mass and ionic diffusion in the electrochemical processes.<sup>1-3</sup> The low viscosity of imprinting inks facilitates the capillary-driven mold filling. By modulating the elastomer stamp dimensions, we create LMO microelectrodes with aspect ratios of 0.7, 1.7 and 3.8 (Figure 1a to 1c). To further improve the aspect ratio, we apply multilayer imprinting strategy to create woodpile-like 3D  $\text{TiO}_2$  microelectrodes, achieving user-defined aspect ratios (Figure 1d-1e). The imprinted woodpile electrodes demonstrate specific capacity of  $250.9 \text{ mAhg}^{-1}$  and stable cycling in a lithium-ion battery. Post-cycling SEM imaging (Figure 1f) shows that the imprinted feature maintain good structural integrity.

Aside from imprinted electrodes, polymer electrolytes that enable solution deposition on electrodes are developed to facilitate microbattery full cell fabrication. The resultant microbattery based on LMO/LTO electrochemical pair demonstrates superior fast charge-discharge capabilities (40% capacity retention at 300 C) and high volumetric power density of  $855 \mu\text{Wcm}^{-2}\mu\text{m}^{-1}$  (Figure 2), which is attributed to the small critical dimension and high surface-to-volume ratio of the imprinted features. In the last part, we will briefly mention about our work of using initiated chemical vapor deposition to optimize the polymer electrolyte coating quality;<sup>4</sup> much better uniformity and conformality can be achieved.

Reference:

- [1]. Li, W.; Christiansen, T. L.; Li, C.; Zhou, Y.; Fei, H.; Mamakhel, A.; Iversen, B. B.; Watkins, J. J., High-power lithium-ion microbatteries from imprinted 3D electrodes of sub-10 nm  $\text{LiMn}_2\text{O}_4/\text{Li}_4\text{Ti}_5\text{O}_{12}$  nanocrystals and a copolymer gel electrolyte. *Nano Energy* **2018**, *52*, 431-440.
- [2]. Li, W.; Zhou, Y.; Howell, I. R.; Gai, Y.; Naik, A. R.; Li, S.; Carter, K. R.; Watkins, J. J., Direct Imprinting of Scalable, High-Performance Woodpile Electrodes for Three-Dimensional Lithium-Ion Nanobatteries. *ACS Appl. Mater. Interfaces* **2018**, *10* (6), 5447-5454.

[3]. Kothari, R.; Beaulieu, M. R.; Hendricks, N. R.; Li, S. K.; Watkins, J. J., Direct Patterning of Robust One-Dimensional, Two-Dimensional, and Three-Dimensional Crystalline Metal Oxide Nanostructures Using Imprint Lithography and Nanoparticle Dispersion Inks. *Chemistry of Materials* **2017**, *29* (9), 3908-3918.

[4]. Li, W.; Bradley, L. C.; Watkins, J. J., Copolymer Solid-State Electrolytes for 3D Microbatteries via Initiated Chemical Vapor Deposition. *ACS Appl. Mater. Interfaces* **2019**, *11* (6), 5668-5674.

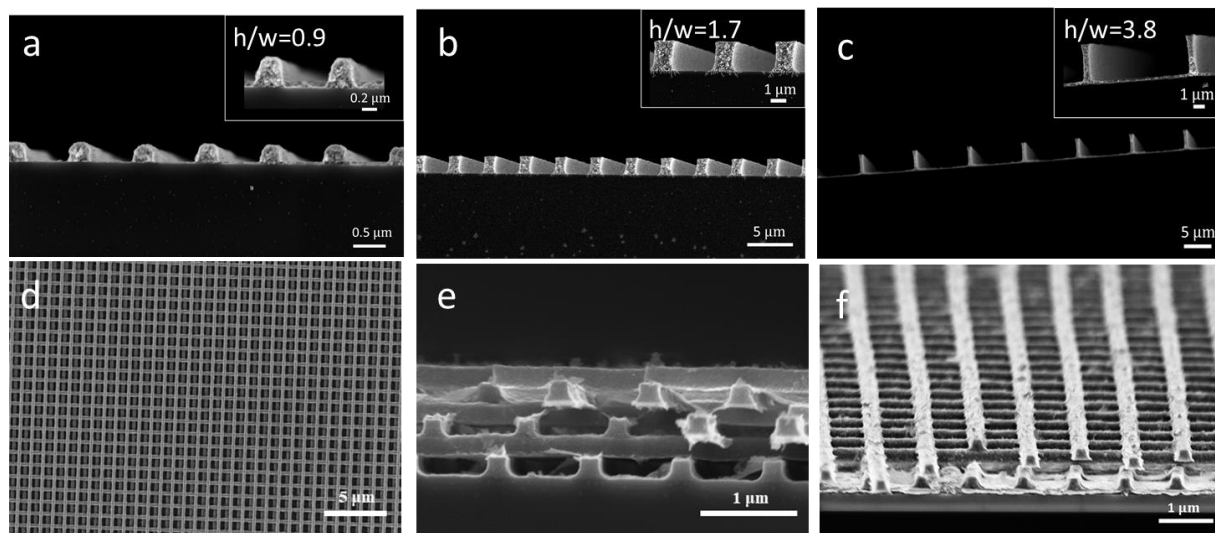


**Figure 1.** (a)-(c) imprinted LMO electrodes with aspect ratios of 0.9, 1.7 and 3.8. (d) and (e) top-down and cross-sectional views of  $\text{TiO}_2$  woodpile electrodes. (f) post-cycling imaging of  $\text{TiO}_2$  woodpile electrode.

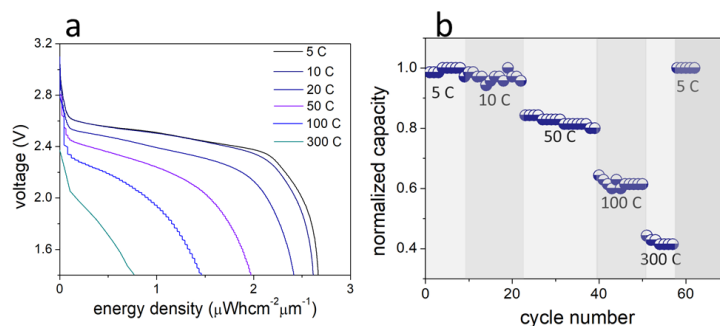


**Figure 2.** (a) discharging profiles of LMO/LTO microbatteries at different C rates. (b) Normalized capacity of micorbattery as a function of C rates and cycle numbers.